Simulation of turbulent dispersion using a simple random model of the flow field

A. D. Jenkins*

Department of Offshore Engineering, Heriot-Watt University, Riccarton, Currie, Edinburgh EH14 4AS, UK
(Received May 1984; revised November 1984)

A method is devised to simulate the movement and spreading of a patch of contaminant in two-dimensional turbulent flow. The turbulent motion is exponentially divided into components of differing wave number, adjacent components being made to have correlation times differing by a factor of two. The turbulent motion is then reconstructed by replacing each component with a sinusoidal advection field having a randomly directed wave number. Contaminant particles are advected by each of the reconstructed components, the smallest scale components being applied first. A computer simulation was performed, using a Kolmogorov $k^{-5/3}$ turbulent energy spectrum. Batchelor's $o \propto t^{3/2}$ law for the spreading of a contaminant patch was reproduced, approximately, as was Richardson's non-Gaussian asymptotic form of the distance-neighbour function.

Key words: simulation, turbulent flow, dispersion, advection

A turbulent flow field is generally a much more effective way of dispersing a contaminant than is molecular diffusion. For example, in the lower atmosphere, the molecular diffusivity is about 2×10^{-5} m^2 s^{-1}, whereas the effective turbulent diffusivity ranges from 10 m^2 s^{-1} when one considers the effect of wind gusts, to 10^7 m^2 s^{-1} when one considers variations in the global circulation.[1] It is this variation in the effectiveness of turbulent motions for dispersion at different scales which prompts one to distinguish between absolute and relative dispersion.

Taylor[2] considered the movement of a 'marked' fluid particle in a turbulent flow. He assumed that the mean flow was zero, and that the turbulence was statistically homogeneous, isotropic and stationary. He found, for length- and time-scales much greater than the largest scales characteristic of the turbulence, that the particle would execute a simple random walk. If the particle is released at time zero and observed at time t, and the experiment repeated many times, the root-mean-square distance that the particle will have moved will be proportional to $t^{1/2}$. This $t^{1/2}$-dependence will also apply to the size of a cluster of particles, if it is assumed that each particle in the cluster moves independently of all the others.

It is false to assume that the contaminant particles in a cluster all move independently if the particles are not all separated by distances which are large compared with the largest turbulence length-scale. If the particles have smaller separations one must consider the concept of relative dispersion: the process of spreading of a patch of contaminant as it moves within the fluid. The spreading will be caused by the turbulent motion on scales of about the same size as the patch and smaller. Motions at larger scales will cause the patch to drift about without significant spreading. As the patch becomes larger, its spreading will become subject to the influence of larger scales of the turbulent motion, and it is this effect which causes the increase in turbulent diffusivity noted by Richardson.[1] If one wishes to investigate the spreading of a patch of contaminant, it is more natural to look initially at the behaviour of the separation:

$$\boldsymbol{y} = \boldsymbol{x}_2 - \boldsymbol{x}_1 \tag{1}$$

of a pair of contaminant particles, rather than the movement of a single particle relative to a fixed origin.

Using Kolmogorov's theory of locally isotropic turbulence, together with associated dimensional analysis arguments, Batchelor[3] showed that:

$$p = \langle |\boldsymbol{y}|^2 \rangle^{1/2} \propto \epsilon^{1/2} t^{3/2} \tag{2}$$

where ϵ is the turbulent energy dissipation rate, and the

*Present address: Continental Shelf Institute, PO Box 1883, N-7001 Trondheim, Norway

0307-904X/85/04239-07/$03.00

time t is measured from a suitably chosen origin, with the angle brackets denoting an ensemble-average. The above equation holds within the 'inertial subrange' of the scales of turbulent motion, where viscous forces are small compared to inertial forces, and where the energy spectrum of the turbulence is given by:

$$E(k) \propto k^{-5/3} \tag{3}$$

where k is the modulus of wave numbers in the Fourier decomposition of the turbulent velocity field.

Equation (2) implies a dispersion coefficient:

$$\frac{1}{2}\frac{\mathrm{d}}{\mathrm{d}t}\langle |y|^2 \rangle \propto \bar{y}^{4/3} \tag{4}$$

There is experimental evidence[6] that the above 4/3-power law is still valid even if the Reynolds number is too small for an inertial subrange to exist.

If one considers a patch of contaminant with concentration $\Gamma(x, t)$, equation (2) can be replaced by:

$$\sigma \propto \epsilon^{1/2} t^{3/2} \tag{5}$$

with the standard deviation:

$$\sigma = \left(\frac{\int |x' - x_0|^2 \Gamma(x', t)\, \mathrm{d}x'}{\int \Gamma(x', t)\, \mathrm{d}x'} \right) \tag{6}$$

where x_0 is the centre-of-mass of the contaminant patch.

Richardson[1] introduced the concept of 'distance-neighbour function' $q(y, t)$. This function describes the distribution of the separation of particle pairs in a contaminant cloud, or ensemble of clouds. $q(y, t)$ is normalized so that it becomes a probability density, i.e.:

$$\int q(y, t)\, \mathrm{d}y = 1 \tag{7}$$

where the integration is over all possible values of the particle separation y. Considering a continuous distribution of contaminant, one has:

$$q(y, t) = \frac{\int \Gamma(x, t)\, \Gamma(x + y, t)\, \mathrm{d}x}{\int \Gamma(x, t)\, \mathrm{d}x} \tag{8}$$

where Γ is the contaminant concentration, and the integrations are over all space.

Richardson proposed that the dispersion of a contaminant cloud could be described by a partial differential equation for the distance-neighbour function:

$$\frac{\partial q}{\partial t} = c_R \nabla_y \cdot (|y|^{4/3} \nabla_y q) \tag{9}$$

where c_R is a constant. On the other hand, Batchelor[5] argued that the effective diffusivity should not depend upon the random separation y, but rather upon a statistical function such as $\bar{y}^{4/3} = \langle |y|^2 \rangle^{2/3}$. Thus equation (9) is changed, to become:

$$\frac{\partial q}{\partial t} = c_B \bar{y}^{4/3} \nabla_y^2 q \tag{10}$$

where c_B is another constant.

A solution for equation (9) is:

$$q(y, t) \propto (c_R t)^{-9/2} \exp\left[-\left(\frac{9|y|^{2/3}}{4 c_R t} \right) \right] \tag{11}$$

whereas, for equation (10), the corresponding solution is the Gaussian distribution:

$$q(y, t) \propto (c_B t)^{-9/2} \exp\left[-\left(\frac{y^2}{2(\frac{2}{3} c_B t)^3} \right) \right] \tag{12}$$

The validity of equation (2) in two-dimensional turbulence is debatable, as the energy spectrum may not obey the Kolmogorov $k^{-5/3}$ law. $E(k)$ may be proportional to k^{-3} (reference 6) or if there is irregular bottom topography, it may be proportional to k^{-1} (references 7 and 8) or may have some other wave number dependence. If $E(k) \propto k^{-3}$, the turbulent dispersion coefficient will be proportional to $\bar{y}^2$, rather than $\bar{y}^{4/3}$, and $\bar{y}$ will increase exponentially with time. If $E(k) \propto k^{-1}$, the turbulent dispersion coefficient will be proportional to $\bar{y}$, and $\bar{y}$ will increase linearly with time.

Modelling turbulent dispersion

The approach adopted by the author in modelling turbulent dispersion is to try to find a method whereby an individual patch of contaminant is followed within a single realization of a turbulent flow. One can then follow, for example, the simulated track of an individual patch of dye, or of an oil slick on the sea surface. Additional effects, such as wind- and wave-induced drift or variations in the background current, should be capable of being incorporated. If ensemble-average statistical quantities are required from such a model, the simulation can be performed a number of times.

In principle, it should be possible to solve numerically the hydrodynamic equations of motion at scales which resolve turbulent 'eddies' of sizes comparable with the initial size of a contaminant patch. Such numerical solutions have indeed been made,[9] but for routine situations they are extremely expensive. Routinely applicable numerical hydrodynamic models will resolve the smooth background variations in the flow field. A practical application of a turbulent dispersion model would be to simulate motions at scales in the range from the initial size of a patch of contaminant up to the scale of the background flow variation.

Before describing the author's turbulent dispersion model, it is useful to review various methods which have been used to model turbulent dispersion.

Eddy-resolving numerical models

As already mentioned, these models are extremely expensive for routine application. They are very useful in fundamental studies of turbulent motion and turbulent dispersion, and in investigating ways of parameterizing the dispersion process for simpler models, which in their turn can be used routinely.

Use of the advection-diffusion equation

If the background flow field $U(x, t)$ is known, from observations or by running a numerical hydrodynamic model, values for the mean concentration $\bar{\Gamma} = \langle \Gamma \rangle$ of a contaminant can be found by solving the advection-diffusion equation:

$$\frac{\partial \bar{\Gamma}}{\partial t} + U \cdot \nabla \bar{\Gamma} = \nabla \cdot \{D(x)\, \nabla \bar{\Gamma}\} \tag{13}$$

where D is a dispersion (diffusion) coefficient. The diffusion term on the right-hand side of (13) will cause a small patch of contaminant to spread with $\sigma \propto t^{1/2}$.

If another time dependence for the spreading is required, e.g. $\sigma \propto t^{3/2}$, a 'spectral diffusion' technique can be used. The spectral diffusion method replaces the diffusion term by:

$$\nabla \cdot \left\{ \int D(\boldsymbol{x}, \boldsymbol{x}') \nabla_{x'} \Gamma \, \mathrm{d}\boldsymbol{x}' \right\} \tag{14}$$

with

$$D(\boldsymbol{x}, \boldsymbol{x}') = \int K(\boldsymbol{k}) \exp[i\boldsymbol{k} \cdot (\boldsymbol{x} - \boldsymbol{x}')] \, \mathrm{d}\boldsymbol{k} \tag{15}$$

(Berkowicz and Prahm[10]). $K(\boldsymbol{k})$ can be of the form, for example:

$$K(\boldsymbol{k}) = \frac{K_0}{1 + B\boldsymbol{k}^{4/3}} \tag{16}$$

which reproduces equation (4) and $\sigma \propto t^{3/2}$ at small scales. In practice, (13) is solved using a pseudo-spectral technique, with the diffusion term evaluated in wave number ($\boldsymbol{k}$) space. Thus, the integrations in (14) and (15) are not performed directly, but indirectly via the fast Fourier transforms used in the pseudo-spectral method.

The spectral diffusion method only gives values for the average concentration at any point. It reproduces neither the greater variations in concentration experienced in turbulent dispersion, nor the advection of the contaminant by motions of smaller scale to that of the background flow field. It is possible to evaluate concentration fluctuations by solving a partial differential equation for the mean square concentration fluctuation ($\overline{\Gamma'^2}$), where $\Gamma' = \Gamma - \bar{\Gamma}$.[11]

Advection of contaminant particles

Instead of treating the contaminant as continuous, one may think of it as being composed of a number of discrete particles, which are advected by the background flow. A patch of contaminant composed of such particles will spread out under the influence of variations in the background flow; but if its initial size is much smaller than the smallest scale of background flow variation, it will tend to spread only very little. This defect may be remedied by forcing a small patch, or small patches, of contaminant to expand according to, for example, the $\sigma \propto t^{3/2}$ or $D \propto y^{4/3}$ law, but it will be difficult, using such a method, to reproduce the essential irregularity and asymmetry of each realization of the turbulent dispersion process.

Random walk methods. Consider a patch composed of a number of discrete particles, as described above. If each particle is allowed to be advected by the background flow, but additionally allowed to make a small random jump at each time step, independently of all other particles and all other time steps, the contaminant patch will spread of its own accord. It is usually sufficient to allow the random jump to have given magnitudes for its x-, y- and z-components (the same magnitude for each coordinate, or different magnitudes for different coordinates, according to whether the turbulence is isotropic or anisotropic), but to have random signs. A contaminant patch will then spread with $\sigma \propto t^{1/2}$; it is difficult to reproduce other types of time dependence. It is, however, very easy to allow the magnitude of the random jumps to vary with position, time, background current etc.[12]

Durbin[13] developed a 'random flight' model for the dispersion of pairs of contaminant particles. For each pair, two 'velocity' time series are constructed, using independent white-noise accelerations, and are then multiplied by functions of the particle separation to obtain the centre-of-mass velocity and the relative particle velocity.

The functions of the particle separation are chosen to give a $D \propto y^{4/3}$ law for the relative dispersion at small scales. Because pairs of particles are considered, the method is unable to simulate directly the dispersion of a patch of contaminant. However, concentration fluctuations can be evaluated by considering two particles close together near position x at time t and running the model backwards in time to determine whether each particle was in the initial contaminant patch. By repeating the process a number of times, the mean concentration and concentration variations at point x at time t can be determined.

Flow field synthesis. Davis[14] performed simulations of the advection of contaminant particles in general flow fields. These consisted of randomly selected realizations of joint normally distributed velocity fields constructed from a large number of Fourier components with randomly selected wave number $\boldsymbol{k}$, each of which had wave-like propagation, i.e. was proportional to $\exp[i(\boldsymbol{k} \cdot \boldsymbol{x} - \omega t)]$. A dispersion relation between $\boldsymbol{k}$ and the frequency ω was prescribed for the whole velocity field. Davis' simulations were therefore of dispersion by random wave fields rather than by turbulent velocity fields, as he did not take into account the advection of the small-scale motions by the larger-scale motions.

In order to include this kind of advection by turbulent flow fields the model described in the following section was devised. It is based on the splitting of the flow field into a 'cascade' of larger and smaller-scale components, and causing the larger-scale components to shear and advect the smaller-scale components.

Simple random model of the flow field

This method was devised for following the movement and spreading of a patch of contaminant in a two-dimensional turbulent flow. It is thus suitable for following, for example, dye patches, or oil slicks which have negligible motion with respect to the underlying water. The fluid flow is assumed for the moment to be two-dimensional, so the method is valid only for scales much greater than the depth of the fluid. If significant depth variations are present, alterations will need to be made to the part of the method which is dependent upon the two-dimensional continuity equation. Alterations also need to be made if regions of convergent or divergent flow are allowed to exist, as in, for example, Langmuir circulation phenomena.

The method is based upon the splitting up of the turbulent motion into components of different wave number, spaced exponentially in wave number magnitude. Each of these different wave number components of the motion has its own characteristic length-scale, velocity and Lagrangian correlation time, and the relationships between these quantities depend upon the assumed turbulent kinetic energy spectrum.

It is assumed that the turbulent flow field is two-dimensional, homogeneous and isotropic, and obeys the continuity equation:

$$\nabla_h \cdot \boldsymbol{u} = \frac{\partial u_x}{\partial x} + \frac{\partial u_y}{\partial y} = 0 \tag{17}$$

Assume further that the flow field possesses an energy

spectrum of the form:

$$E(k) = Ak^{-\gamma} \qquad \tfrac{1}{2}\langle |u|^2 \rangle = \int_0^\infty E(k)\,\mathrm{d}k \tag{18}$$

where k is the magnitude of the wave number vector $\boldsymbol{k}$. The parameter γ may be 5/3, as in the Kolmogorov energy cascade spectrum,[15] or may take different values, such as 3, for the enstrophy cascade spectrum,[6] or 1, as predicted by Herring[7] for flow over irregular bottom topography, and observed by Veth and Zimmerman.[8]

The turbulent flow field is now divided into components,[16,17] each component having wave numbers in the range $k_{1/2} > k \geqslant k_{3/2}$, $k_{3/2} > k \geqslant k_{5/2}$ etc., with the $k_{m+(1/2)}$ in geometric ratio, $k_{m-(1/2)} = bk_{m+(1/2)}$, for integers m. If the characteristic wave numbers are defined:

$$k_m = (k_{m-(1/2)}k_{m+(1/2)})^{1/2} \tag{19a}$$

characteristic length-scales:

$$l_m = k_m^{-1} = b^{m-1}l_1 \tag{19b}$$

characteristic velocities:

$$u_m = \left\{ 2A \int_{k_m+\frac{1}{2}}^{k_m-\frac{1}{2}} k^{-\gamma}\,\mathrm{d}k \right\}^{1/2}$$

$$= \left\{ \frac{2A}{\gamma-1} k_m^{1-\gamma}(b^{(\gamma-1)/2} - b^{(1-\gamma)/2}) \right\}^{1/2} \qquad \text{for } \gamma \neq 1 \tag{20}$$

$$= \{2A \ln b\}^{1/2} \qquad \text{for } \gamma = 1$$

and characteristic time intervals (assumed equal to the Lagrangian correlation time for each component of the flow):

$$T_m = (u_m k_m)^{-1} \tag{21}$$

For each component, a velocity field is synthesized:

$$\boldsymbol{u}_m(\boldsymbol{x}) = \mathrm{Re}\{u_m \hat{\boldsymbol{u}}_m \exp[i(k_m \hat{\boldsymbol{k}}_m \cdot \boldsymbol{x} + \phi_m)]\} \tag{22}$$

where $\hat{\boldsymbol{u}}_m$ and $\hat{\boldsymbol{k}}_m$ are randomly directed unit vectors, and ϕ_m is a random phase, uniformly distributed on $[0, 2\pi)$. The continuity equation (17) requires:

$$\hat{\boldsymbol{u}}_m \cdot \hat{\boldsymbol{k}}_m = 0 \tag{23}$$

The principle of the method is that contaminant particles are advected by the component $\boldsymbol{u}_m$ of the flow for a time T_m, and that the smaller-scale components operate on the particles before the larger-scale components. The ratio of adjacent length-scales, b, is chosen so that $T_{m+1} = 2T_m$ (or, alternatively, another integer multiple). Thus:

$$u_{m+1}k_{m+1} = \tfrac{1}{2}u_m k_m \tag{24}$$

from which one obtains:

$$b^{(3-\gamma)/2} = 2$$

i.e.

$$b = 2^{2/(3-\gamma)} \qquad \text{for } \gamma \neq 3 \tag{25}$$

If $\gamma \to 3$, $b \to \infty$, but then T_m is found to be independent of m, it being a function of A and b only.

From equations (20) and (21) the following are obtained for $\gamma \neq 1$, $\gamma \neq 3$:

$$T_m = \left(\frac{2A}{\gamma-1}\right)^{-1/2} b^{(\gamma-1)/4}(1-b^{1-\gamma})^{-1/2} k_m^{-(3-\gamma)/2} \tag{26}$$

Hence:

$$k_m = \left\{ \left(\frac{2A}{\gamma-1}\right)^{1/2} b^{(\gamma-1)/4}(1-b^{1-\gamma})^{1/2} T_m \right\}^{-2/(3-\gamma)} \tag{27}$$

and u_m can be evaluated from (21).

If one now starts from time zero with a patch of contaminant particles with coordinates $\boldsymbol{x}_j(0)$, their positions at time nT_1 are determined by the following procedure. Define the 'pseudo-position' $\boldsymbol{x}'_j(T_1)$ by:

$$\boldsymbol{x}'_j(T_1) = \boldsymbol{x}_j(0) + \boldsymbol{u}_1^{(1)}\{\boldsymbol{x}_j(0)\}\,T_1 \tag{28}$$

where $\boldsymbol{u}_m^{(1)}$, $\boldsymbol{u}_m^{(2)}$ etc. are realizations of the velocity field $\boldsymbol{u}_m$, defined in equations (22) and (23) with independent values of the random wave number-directions $\hat{\boldsymbol{k}}_m$ and phases ϕ_m. From each set of pseudo-positions $\boldsymbol{x}'_j((p-1)T_1)$ the next set of pseudo-positions $\boldsymbol{x}'_j(pT_1)$ is obtained by advection by the velocity field $\boldsymbol{u}_1^{(p)}$ first, then $\boldsymbol{u}_2^{(p/2)}$, $\boldsymbol{u}_3^{(p/4)}$ etc. in succession, terminating with:

$$\boldsymbol{u}_Q^{(p/2^{Q-1})}$$

where:

$$p \equiv 0 \pmod{2^{Q-1}} \qquad p \not\equiv 0 \pmod{2^Q} \tag{29}$$

or the largest scale velocity field $\boldsymbol{u}_L^{(p/2^{L-1})}$, if $Q > L$.

The reason that the smaller-scale components operate first is that in general the time-scales T_m are shorter for the smaller-scale components. Thus, within the time interval in which one random realization of a large-scale component acts, there will be many successive operations by independent realizations of a small-scale component. If one were to operate with the larger-scale components first, one would be unable to simulate the effect of the advection of the smaller-scale components of the velocity field by the larger-scale components.

The pseudo-positions $\boldsymbol{x}'_j(pT_1)$ do not, however, contain the effects of advection by motion at scales larger than $l_Q = 1/k_Q$, where Q is defined in (29). To obtain the actual simulated positions for times not equal to an integer multiple of the largest characteristic time scale T_L, one needs to operate on the $\boldsymbol{x}'_j(pT_1)$ with the velocity fields $\boldsymbol{u}_{Q+1}, \boldsymbol{u}_{Q+2}, \ldots, \boldsymbol{u}_L$, taking into account the fact that these velocity fields will only operate for the appropriate fractions of the time scales $T_{Q+1}, T_{Q+2}, \ldots, T_L$.

The above procedure can be expressed in terms of successive applications of advection operators $\alpha\{\boldsymbol{u}, T\}$, where:

$$\alpha\{\boldsymbol{u}, T\}\,\boldsymbol{x} = \boldsymbol{x} + \boldsymbol{u}(\boldsymbol{x})\,T \tag{30}$$

The procedure for advection by the simulated turbulent flow is as follows:

$$\begin{aligned} &(1) \quad \boldsymbol{x}'_j(T_1) = \alpha\{\boldsymbol{u}_1^{(1)}, T_1\}\boldsymbol{x}_j(0) \\ &(2) \quad \boldsymbol{x}'_j(pT_1) = \alpha\{\boldsymbol{u}_\lambda^{(p/2^{\lambda-1})}, T_\lambda\}\,\alpha\{\boldsymbol{u}_{\lambda-1}^{(p/2^{\lambda-2})}, T_{\lambda-1}\} \\ &\qquad \ldots \alpha\{\boldsymbol{u}_1^{(p)}, T_1\}\boldsymbol{x}'_j(p-1)T_1) \end{aligned} \tag{31}$$

where λ is L or the greatest integer such that p is divisible by $2^{\lambda-1}$, whichever is the smaller.

$$x_j'(pT_1) \quad \text{if } p \text{ is divisible by } 2^{L-1}$$

$$(3)\quad x_j(pT_1) = \alpha\{u_L^{(I_L)}, R_L T_1\}\alpha\{u_{L-1}^{(I_{L-1})}, R_{L-1}T_1\} \quad (32)$$

$$\ldots\alpha\{u_{\lambda+1}^{(I_{\lambda+1})}, R_{\lambda+1}T_1\}x_j'(pT_1) \text{ otherwise}$$

where I_s is the integer part of $p/2^{s-1}$, and R_s is the remainder after p is divided by 2^{s-1}.

It should be noted that since the values of $\hat{k}_m$ and ϕ_m at successive T_m-intervals are independent, the value of $u_m(x)$ will change after time steps which are integer multiples of T_m. This will cause kinks to appear in particle paths at intervals of $2^{m-1}T_1$, the kinks in general becoming stronger for larger values of m. It may perhaps be possible to eliminate the kinks by performing some kind of smooth interpolation between the values of u_m at successive T_m intervals.

In principle, it is possible to construct a simulated turbulence field using distortions at different scales which are different from the sinusoidal distortions given by (22), (23) and (30); for example, one may try to simulate the distortions caused by circular eddies. If the continuity equation is to be obeyed, the advection operators α must preserve the Jacobian, i.e.:

$$\frac{\partial(\alpha x)}{\partial(x)} \equiv \frac{\partial(\alpha x)_x}{\partial x}\cdot\frac{\partial(\alpha x)_y}{\partial y} - \frac{\partial(\alpha x)_x}{\partial y}\cdot\frac{\partial(\alpha x)_y}{\partial x} = 1 \quad (33)$$

Computer simulation

For the computer simulation of two-dimensional turbulent dispersion, a zero mean flow has been assumed, with a turbulent energy spectrum given by:

$$E(k) = 0.5k^{-5/3} \quad (34)$$

The characteristic time interval T_1 of the smallest scale component was taken to be 1.0 units, and the largest scale characteristic time interval, T_6, was 32 units. The corresponding length scales l_1 and l_6 are given by:

$$l_m = (3^{1/2}2^{-1/4}A^{1/2}T_m)^{3/2} = (1.03\,T_m)^{3/2} \quad (35)$$

(from (27) and (34)). Hence the smallest length-scale $l_1 = 1.05$, and the largest length-scale $l_6 = 189$. If the proportionality constant A in the energy spectrum is changed from its value of 0.5 in equation (34), this will alter each l_m as a function of the T_m: the length-scales will increase as A increases.

Figure 1 shows the movement of the centre-of-mass of a patch of contaminant containing 80 particles, initially circular with diameter 10 units. *Figures 2* and *3* show the evolution of the patch itself, at twice the scale of *Figure 1*, with the centre-of-mass of the patch as origin. In *Figures 2b*, *2c* and *3*, the patch shows irregularities at both large and small scales – this phenomenon is to be expected if the patch is advected by turbulent motions. If each particle in the patch were to move independently of all the others, the general shape of the patch would be expected to maintain the initial circular symmetry.

Figure 4 shows the evolution with time of the ensemble-average variance of the contaminant patch:

$$\langle\sigma^2(t)\rangle = \frac{1}{N}\sum_j |x_j(t) - x_0(t)|^2$$

$$\text{for } 0 < t \leqslant 400 \quad (36)$$

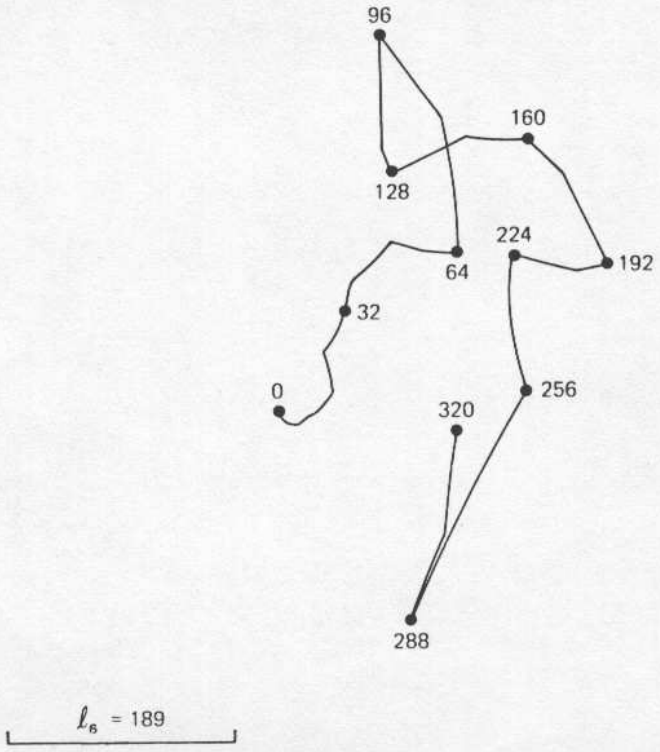

Figure 1 Movement of centre-of-mass of a patch of contaminant, initially circular with diameter 10 units, during 320 unit time steps. The size of l_6, the largest length-scale of motion, is marked; the largest time-scale, T_6, is 32 units

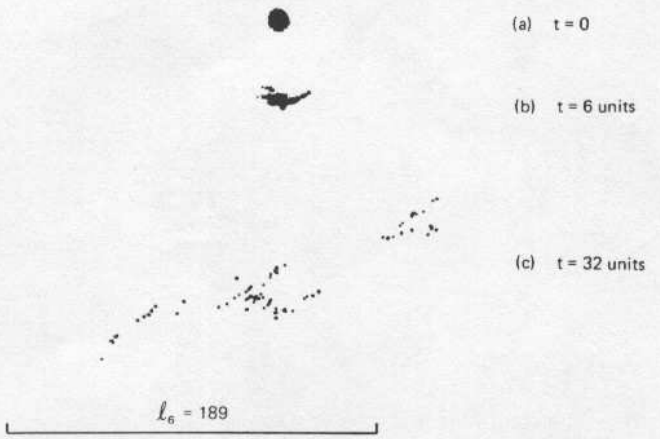

Figure 2 (a), Initial contaminant patch; (b), contaminant patch at $t = 6$; (c), contaminant patch at $t = 32$; scale is twice the scale of *Figure 1*

where the summation is over all particles, N is the total number of particles, and x_0 is the centre-of-mass of the patch. The ensemble-average is taken over 15 simulation runs with 80-particle patches as in *Figures 1-3*. The straight line is obtained by a three-parameter nonlinear least-squares fit, minimizing the quantity:

$$\sum_{t=1}^{225}\frac{1}{t+t_0}\left[\ln\langle\sigma^2(t)\rangle - \zeta\ln(t+t_0) - \ln C\right]^2 \quad (37)$$

with respect to t_0, ζ and C, i.e. the straight line represents:

$$\langle\sigma^2\rangle = C(t+t_0)^{\zeta} \quad (38)$$

The computer simulation was performed on the Honeywell 66 installation at Aberdeen University, the 15 simulation

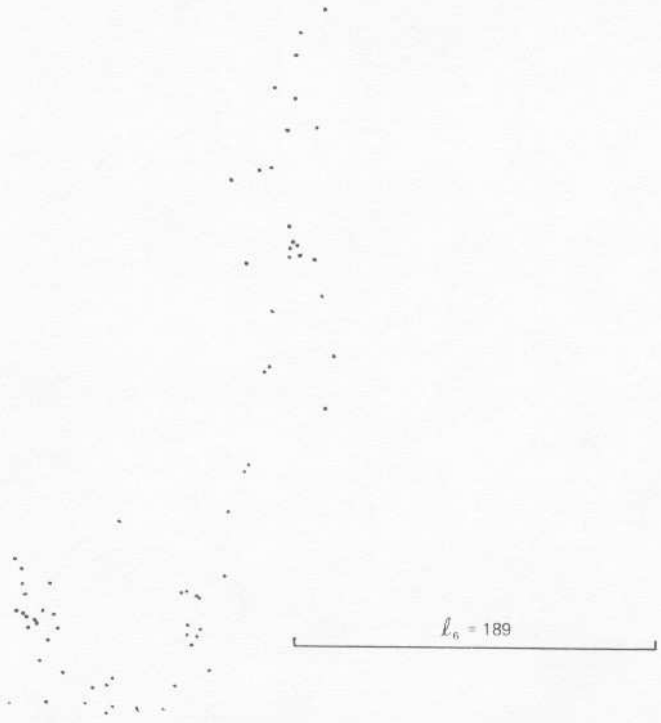

Figure 3 Contaminant patch at $t = 128$ (scale as *Figure 2*)

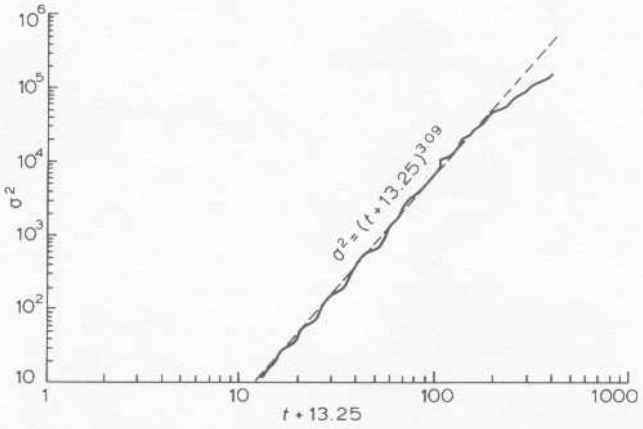

Figure 4 Plot of ensemble-average variance of contaminant patch (15 simulation runs) against (time + t_0) — least-squares fit to straight line $\sigma^2 = C(t + t_0)^{\zeta}$, with C, t_0, ζ as adjustable parameters

runs with six scales of motion and 80 particles taking a total of approximately 10 min of CPU time. The computational algorithms were not optimized for fast running, so there is the prospect of a considerable reduction in run time.

The cut-off limit $t = 225$ was chosen because if a larger upper limit were used (say $t = 400$), $\langle\sigma^2\rangle^{1/2}$ would become much greater than l_6, the largest scale characteristic of the turbulence, and the theoretical power law $\sigma \propto (t + t_0)^{3/2}$ would not be valid. It can be seen that the graph of $\langle\sigma^2\rangle$ departs considerably from the straight line predicted by (38) for large values of t.

In *Figure 4*, it is seen that $t_0 = 13.2$, $\zeta = 3.1$ and $C = 4.6 \times 10^{-3}$. When further simulation runs were performed, the value of the exponent ζ ranged from 2.4 to 3.2; a considerable variation. From this one can say that the results of the simulation are not inconsistent with the $\sigma^2 \propto t^3$ ($\sigma \propto t^{3/2}$) law, but that for a small number of runs, the results show considerable variation. Certainly, a time dependence completely different from $\sigma \propto t^{1/2}$ is produced. It is interesting to note that Okubo's[18] survey of oceanographic field observations gives a value of the exponent ζ equal to 2.34, close to the lower end of the range given by the computer simulations.

A version of Richardson's distance-neighbour function was also calculated, using the computer simulation method on an ensemble of 900 particle pairs, each separated initially by five units. A probability distribution was obtained for the particle separation $y = |y|$, with probability density function:

$$S(y, t) = \frac{1}{2\pi} \int_0^{2\pi} q((y \cos\theta, y \sin\theta), t)\, \mathrm{d}\theta \tag{39}$$

where $q(y, t)$ is the distance-neighbour function defined earlier (equation (7)). The Richardson and Batchelor asymptotic expressions (11)-(12) for the distance-neighbour function become:

$$S_R(y, t) = \frac{20y}{\langle y^2(t)\rangle} \exp\left\{-\left(\frac{60y^2}{\langle y^2(t)\rangle}\right)^{1/3}\right\} \tag{40}$$

and

$$S_B(y, t) = \frac{2y}{\langle y^2(t)\rangle} \exp\left\{-\frac{y^2}{\langle y^2(t)\rangle}\right\} \tag{41}$$

where the time evolution has been incorporated into the ensemble-averages $\langle y^2(t)\rangle$.

Figure 5 shows the evolution of $S(y, t)$ with $t = 1$, $t = 8$ and $t = 64$. In each case, the horizontal axis is scaled so that $\langle y^2\rangle^{1/2} = 1$. On this scale, the distribution for $t > 64$ does not change in form, i.e. by the time $t = 64$, an asymptotic form for the distance-neighbour function has been reached. The Richardson and Batchelor expressions are shown in both figures, and it can be seen that the

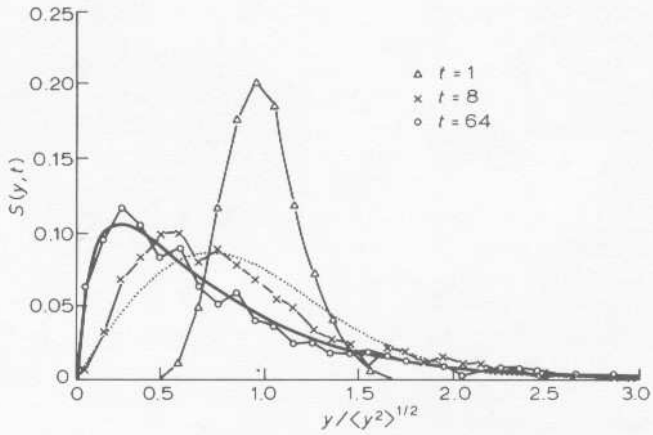

Figure 5 Two-dimensional radial distance-neighbour function $S(y, t)$ for 900 simulation runs of particle pairs. Horizontal scale, 1.0 = one standard deviation; triangles, $t = 1$; crosses, $t = 8$; circles, $t = 64$. Continuous curve, Richardson expression; dotted curve, Batchelor expression (two-dimensional radial Gaussian)

Richardson expression appears to be a better approximation to the asymptotic distance-neighbour function. This result is in apparent contrast to the experimental observations made by Sullivan[19]; however, inspection of Sullivan's results does show a distance-neighbour function which is intermediate between the Richardson and Batchelor expressions.

Conclusions

The simple random model of turbulence described in this paper, based upon the idea of exponentially dividing the length- and time-scales of the turbulent motion, appears to provide a realistic means of simulating two-dimensional turbulent dispersion. If the Kolmogorov $k^{-5/3}$ energy spectrum is assumed, the $\sigma \propto t^{3/2}$ power law for turbulent dispersion is obeyed approximately, and the Richardson asymptotic form of the distance-neighbour function is produced. The model is capable of being modified to fit other turbulent energy spectra, and it should be possible to extend the model to three dimensions, and to apply it to situations where the turbulence is inhomogeneous.

Acknowledgements

This work was conducted at the Department of Offshore Engineering Heriot-Watt University, Edinburgh, while the author was in receipt of a Research Associateship sponsored by the UK Science and Engineering Research Council under the Marine Technology programme. The paper was prepared for publication at the Continental Shelf Institute, Trondheim, with support from the Royal Norwegian Council for Scientific and Technical Research.

Nomenclature

A	constant
b	ratio of adjacent characteristic wave numbers
B	constant
c_B	constant
c_R	constant
C	estimated dispersion intensity
D	dispersion coefficient
$E(k)$	turbulent energy spectrum
i	$\sqrt{-1}$
I_s	integer part of $p/(2^{s-1})$
$\boldsymbol{k}$	wave number vector in Fourier decomposition of velocity field or other spatial field
k	modulus of wave number vector
k_m	mth characteristic wave number
$\hat{\boldsymbol{k}}_m$	random unit vector
$K(\boldsymbol{k})$	spectral dispersion coefficient
K_0	constant
L	index number of largest scale of motion
l_m	mth characteristic length-scale
p	an integer
$q(\boldsymbol{y}, t)$	Richardson's distance-neighbour function
Q	an integer
R_s	remainder after p is divided by 2^{s-1}
$S(\boldsymbol{y}, t)$	probability density function for particle separation
$S_B(\boldsymbol{y}, t)$	Batchelor's expression for $S(\boldsymbol{y}, t)$
$S_R(\boldsymbol{y}, t)$	Richardson's expression for $S(\boldsymbol{y}, t)$
s	an integer
t	time
t_0	estimated power law dispersion time origin offset
T_m	mth characteristic time interval
$\boldsymbol{U}$	background flow-field velocity (deterministic: obtained from observations or a deterministic model)
$\boldsymbol{u}$	velocity vector (general: can be deterministic or random)
u_m	mth characteristic velocity
$\boldsymbol{u}_m$	random velocity field at scale m
$\boldsymbol{u}_L$	largest-scale random velocity field
$\hat{\boldsymbol{u}}_m$	random unit vector
$u_m^{(p)}$	pth realization of random velocity field at scale m
$\boldsymbol{x}, \boldsymbol{x}'$	position vectors
$\boldsymbol{x}_0$	centre-of-mass of contaminant patch
$\boldsymbol{x}_j(t)$	position of the jth particle at time t
$\boldsymbol{x}'_j(t)$	pseudo-position of jth particle at time t
$\boldsymbol{y}$	particle separation vector
y	$\lvert\boldsymbol{y}\rvert$
$\bar{y}$	$\langle\lvert\boldsymbol{y}\rvert^2\rangle^{1/2}$
$\alpha\{\boldsymbol{u}, t\}$	advection operator
γ	energy spectrum exponent
Γ	contaminant concentration
$\bar{\Gamma}$	mean contaminant concentration
Γ'	concentration fluctuation
ϵ	turbulent energy dissipation rate
ζ	estimated dispersion exponent
θ	an angle
λ	an integer
σ	standard deviation size of a contaminant patch
ϕ_m	random phase
ω	frequency
∇	gradient operator
$\nabla\cdot$	divergence operator
$\nabla_h\cdot$	horizontal divergence operator
∇_y	gradient operator in $\boldsymbol{y}$-space
(a_x, a_y)	two-dimensional vector $\boldsymbol{a}$
$\langle\cdot\rangle$	ensemble average
$[0, 2\pi)$	interval $0 \leqslant \phi < 2\pi$
a_x, a_y etc.	x-, y- etc. components of vector $\boldsymbol{a}$
$\boldsymbol{a}\cdot\nabla$	$a_x\dfrac{\partial}{\partial x} + a_y\dfrac{\partial}{\partial y} + a_z\dfrac{\partial}{\partial z}$
$a \equiv 0 \pmod b$	a is divisible by b
$a \not\equiv 0 \pmod b$	a is not divisible by b

References

1 Richardson, L. F. *Proc. Roy. Soc. London* 1926, **A110,** 709
2 Taylor, G. I. *Proc. London Math. Soc., 2nd series* 1921, **20,** 196
3 Batchelor, G. K. *Quart. J. Roy. Meteorol. Soc.* 1950, **76,** 133
4 Sullivan, P. J. *Mém. Soc. R. Sci. Liège, 6e série* 1975, **7,** 253
5 Batchelor, G. K. *Proc. Cambridge Philos. Soc.* 1952, **48,** 345
6 Kraichnan, R. H. *Phys. Fluids* 1967, **10,** 1417
7 Herring, J. R. *J. Atmos. Sci.* 1977, **34,** 1731
8 Veth, C. and Zimmerman, J. T. F. *J. Phys. Oceanogr.* 1981, **11,** 1425
9 Holloway, G. *Ocean Modelling* 1982, **43,** 5 (unpublished manuscript)
10 Berkowicz, R. and Prahm, L. P. *J. Appl. Meteorol.* 1979, **18** 266
11 Csanady, G. T. *J. Atmos. Sci.* 1967, **24,** 21
12 Allen, C. M. *Proc. Roy. Soc. London* 1982, **A389,** 179
13 Durbin, P. A. *J. Fluid Mech.* 1980, **100,** 279
14 Davis, R. E. *J. Mar. Res.* 1983, **41,** 163
15 Batchelor, G. K. *Proc. Cambridge Philos. Soc.* 1947, **43,** 534
16 Frisch, U., Salem, P. L. and Nelkin, M. *J. Fluid Mech.* 1978, **87,** 719
17 Benzi, R., Vitaletti M. and Vulpiani, A. *J. Phys. A: Math. Gen.* 1982, **15,** 883
18 Okubo, A. *Deep-Sea Res.* 1971, **18,** 789
19 Sullivan, P. J. *J. Fluid Mech.* 1971, **47,** 601